OPERATIONAL EXPERIENCE WITH A 100 kW SOLAR PILOT PLANT FOR THERMAL DISSOCIATION OF ZINC OXIDE

Christian Hutter[1], Willy Villasmil[1], Marc Chambon[1], Anton Meier[1]

[1] Solar Technology Laboratory, Paul Scherrer Institute, 5232 Villigen PSI, Switzerland

Phone: +41 56 310 27 88; Fax: +41 56 310 31 60; E-mail: anton.meier@psi.ch

Abstract

Solar H_2 and syngas are produced via a two-step H_2O/CO_2-splitting thermochemical cycle based on Zn/ZnO redox reactions. This closed cycle consists of: (1) the endothermic dissociation of ZnO to Zn and O_2 at 2000 K, using concentrated solar energy; (2) the non-solar exothermic re-oxidation of Zn with H_2O and/or CO_2 to H_2 and/or CO, while the initial metal oxide, ZnO, is recycled to the first step. Based on a 10 kW prototype concept, a 100 kW solar reactor has been designed and fabricated at PSI. The reactor features a rotating cavity lined with ZnO particles that are directly exposed to concentrated solar radiation entering through a transparent quartz window. A screw conveyor allows the semi-batch-wise addition of ZnO particles into the reactor cavity throughout the duration of the experiment. Testing of the pilot plant was performed at the 1 MW Solar Furnace (MWSF) of PROMES-CNRS in Odeillo, France. A description of the solar pilot plant layout including the solar reactor technology, initial operational experience and preliminary results from work in progress is presented.

Keywords: Solar energy; thermochemical cycle; chemical reactor; ZnO dissociation; hydrogen; syngas.

1. Introduction

Energy availability and global warming related to anthropogenic carbon dioxide emissions are current key challenges. Solar processes for the production of storable and transportable chemical fuels ("solar fuels") can contribute to solving these challenges by decreasing the fossil fuels consumption and, consequently, the CO_2 emissions [1]. Hence, PSI's Solar Technology Laboratory has been focusing its research on thermochemical cycles based on metal oxide redox reactions to produce hydrogen (H_2) [2] and – more recently – synthesis gas (H_2+CO). Syngas represents the building block for a wide variety of synthetic fuels, including Fischer-Tropsch liquid fuels (primarily diesel and jet fuel), that are required to power the transportation sectors [3]. Producing high-quality syngas with concentrated solar energy from H_2O and CO_2 – the latter eventually captured from air – represents a viable path towards sustainable energy utilization [4].

The Zn/ZnO redox pair emerges as one of the most promising for solar-driven H_2O and CO_2 splitting cycles [5]. This closed cycle consists of two separate steps, shown schematically in Fig. 1. In the first step, ZnO is endothermally dissociated at high temperature (ca. 2000 K) via concentrated solar radiation, yielding gaseous Zn and O_2. The product gases are quenched with argon (Ar) at the reactor exit to obtain solid Zn and decrease parasitic re-oxidation [6]. In the second step, the collected Zn reacts exothermally with H_2O and/or CO_2 (typically below 1000 K), yielding H_2 and/or CO and ZnO, the latter being recycled back to the solar reactor. This paper focuses on the solar reactor technology required for the first step. Experimental investigations with a 10 kW reactor prototype have led to solar-to-chemical efficiencies as high as 3.1 % [7]. The experimental data allowed validating a heat transfer model, predicting solar-to-chemical efficiencies of up 50.0 % and 55.9 % for similarly designed reactors at the 100 kW and 1000 kW scales, respectively [4]. These promising results were the motivation to design, build and test a 100 kW scale-up version of the 10 kW solar reactor in order to demonstrate the technical feasibility and assess the predicted reactor performance. The 100 kW solar pilot plant was tested in June/July 2011 at the 1 MW Solar Furnace (MWSF) of PROMES-CNRS in Odeillo, France [8]. In this paper, a description of the solar pilot plant layout including the solar reactor technology, initial operational experience and preliminary results from work in progress is presented.

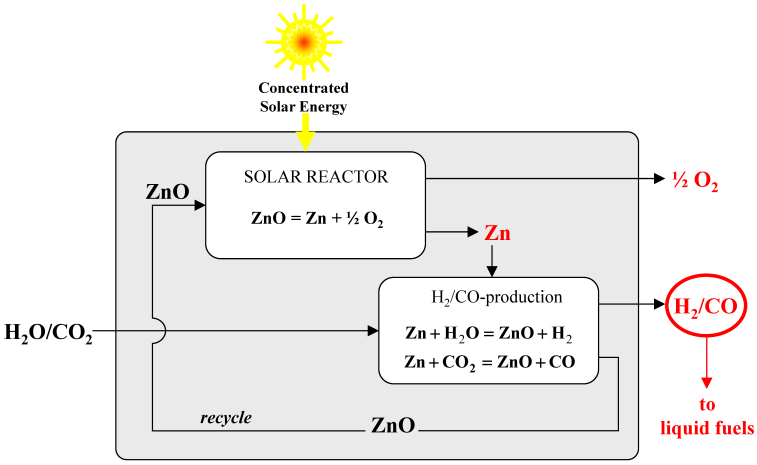

Fig. 1. Schematic of the two-step solar thermochemical cycle based on Zn/ZnO redox reactions to produce H_2 and/or CO from H_2O and/or CO_2 [5].

2. The 100 kW solar pilot plant

2.1. Solar reactor technology

The design of the 100 kW solar pilot reactor as depicted in Fig. 2a is based on previously investigated 10 kW reactor prototypes [9]-[11]. The hexagonal reactor shell is made of a 5 mm thick aluminum sheet to keep low the overall reactor weight. The shell consists of four divisible parts with the aim of allowing access to the reactor cavity and simplifying maintenance tasks: (1) The water-cooled front cone is attached to (2) the front cap, followed by (3) the center casing with the well-insulated cavity and (4) the rear panel containing the water-cooled quench unit. The total length of the reactor shell is 1327 mm and its minimum outer diameter is 1090 mm. The reactor shell is lined with four layers of refractory ceramics (Insultech AG), shown in Fig. 2b. The outermost layer (L4) is 20 mm thick porous insulation consisting of 69 % SiO_2 and 30 % SiC, followed by a 165 mm thick layer (L3) of alumina silicate fiber (55 % Al_2O_3, 40 % SiO_2, T_{max} = 1673 K) and a subsequent 50 mm thick layer (L2) made of 90 % Al_2O_3 and 8 % SiO_2 (T_{max} = 2073 K). The reactor assembly is finished with 12.7 mm thick sintered alumina tiles consisting of 99.5 % Al_20_3 (L1), hold in position with high temperature adhesive (Kerathin P1800, 84 % Al_2O_3, 16 % SiO_2, T_{max} = 2073 K, Rath AG). This results in an inner cavity diameter of 580 mm and a length of 750 mm. The maximum cavity temperature is limited by the ZnO-Al_2O_3-SiO_2 eutectic phase melting temperature at around 1930 K [12].

Concentrated solar radiation is entering the cavity through a frustum-shaped (45°) front cone with an aperture diameter of 190 mm, as depicted in Fig. 2a. The water-cooled copper cone is coated with a 1 mm thick ZrO_2 layer and finished with a 0.5 mm thick Al_2O_3 layer (Sulzer Metco Ltd.). This ceramic coating increases the cone surface temperature with the aim of avoiding undesirable condensation of product gases on its surface, introducing hot gas flows towards the quartz window. This transparent window with a diameter of 600 mm and a thickness of 12 mm closes the reactor from the surroundings and is hold in place by a water-cooled aluminum reactor front shield. To protect the window, an aerodynamic curtain is formed by injecting Ar through 12 radial nozzles at the window and 24 tangential nozzles embedded in the middle of the coated frustum-shaped cone. The benefit of the Ar flow is two-fold: it reduces the Zn condensation on the window and acts as a carrier for the evolving gaseous products. The outlet of the reactor is an annular clearance in the center of the rear panel formed by a circular opening with a diameter of 105 mm and the ZnO particle feeder (Messag AG) with an outer tube diameter of 80 mm. The ZnO particles are fed from a container by a water-cooled conveyor screw, as shown in Fig. 3. During feeding, the conveyor screw moves horizontally into the cavity to distribute the ZnO powder along the bottom of the cavity. In the water-cooled quench unit, based on

the concept presented in [11] and located at the outlet of the reactor cavity, up to 1500 l_N[1]/min of Ar can be added to the reacting gas flow coming from the cavity. The cold quench gas flow is injected through a circular ring gap with an angle of 10 degrees towards the flow to rapidly cool the reacting gas stream below the Zn melting point (693 K), thus favoring the formation of solid Zn particles and reducing the re-oxidation of Zn [6].

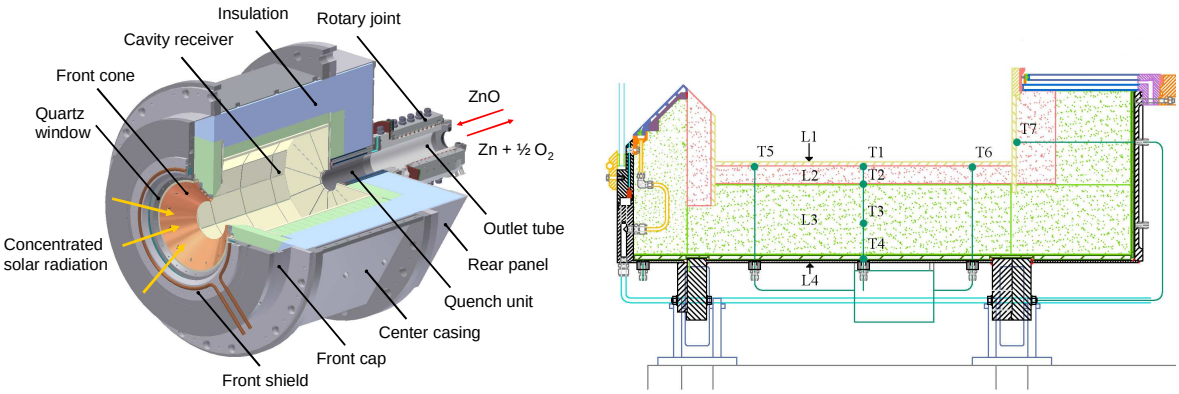

a) b)

Fig. 2. a) Schematic of the 100 kW solar reactor; b) Schematic cross-sectional view of the lower part of the reactor with various thermocouples (T_i) and different insulation layers (L_i) indicated.

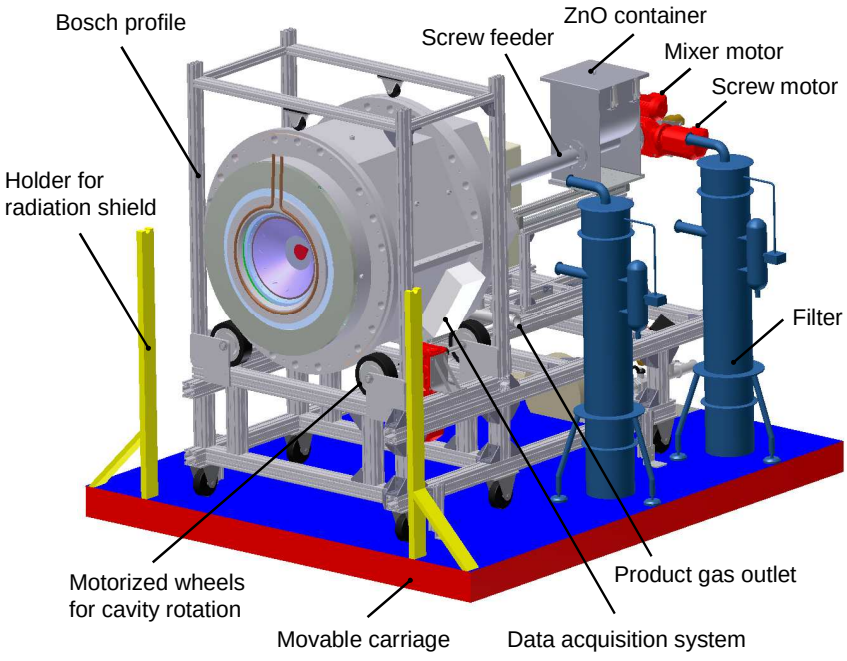

Fig. 3. 3D schematic view of the 100 kW solar pilot plant mounted on the movable carriage, including the solar reactor, the dynamic screw feeder, and the filter system.

[1] l_N refers to liters at standard conditions: 273 K and 1 atm.

2.2. Solar plant layout

Figure 4 shows the layout of the solar pilot plant. The process control system is running on a computer located in the control room of the MWSF, using hardware (real-time controller cRIO-9012) and software (Labview) from National Instruments. Three webcams are mounted on the tower platform to survey the solar pilot plant during operation. A high-resolution camera is placed opposite the solar tower at a distance of 18 m from the focal plane to continuously monitor the reactor front and the cavity. It is capable of recording in real time the evolution of vapor inside the cavity and any precipitations on the window, as well as incidents occurring during experimentation.

A water-cooled radiation shield stands in front of the reactor to collect the spillage radiation and to allow solar radiation to pass trough a circular opening of 600 mm diameter corresponding to the window diameter of the solar reactor. The cooling system further comprises the water-cooled feeder and various water-cooled components on the rotary reactor (front shield, front cone, and quench unit) that are accessed via a rotary joint. The cooling water (CW) supply to all cooled components runs through an open circuit and is monitored by flow meters (GEMÜ GmbH) mounted on the CW rack.

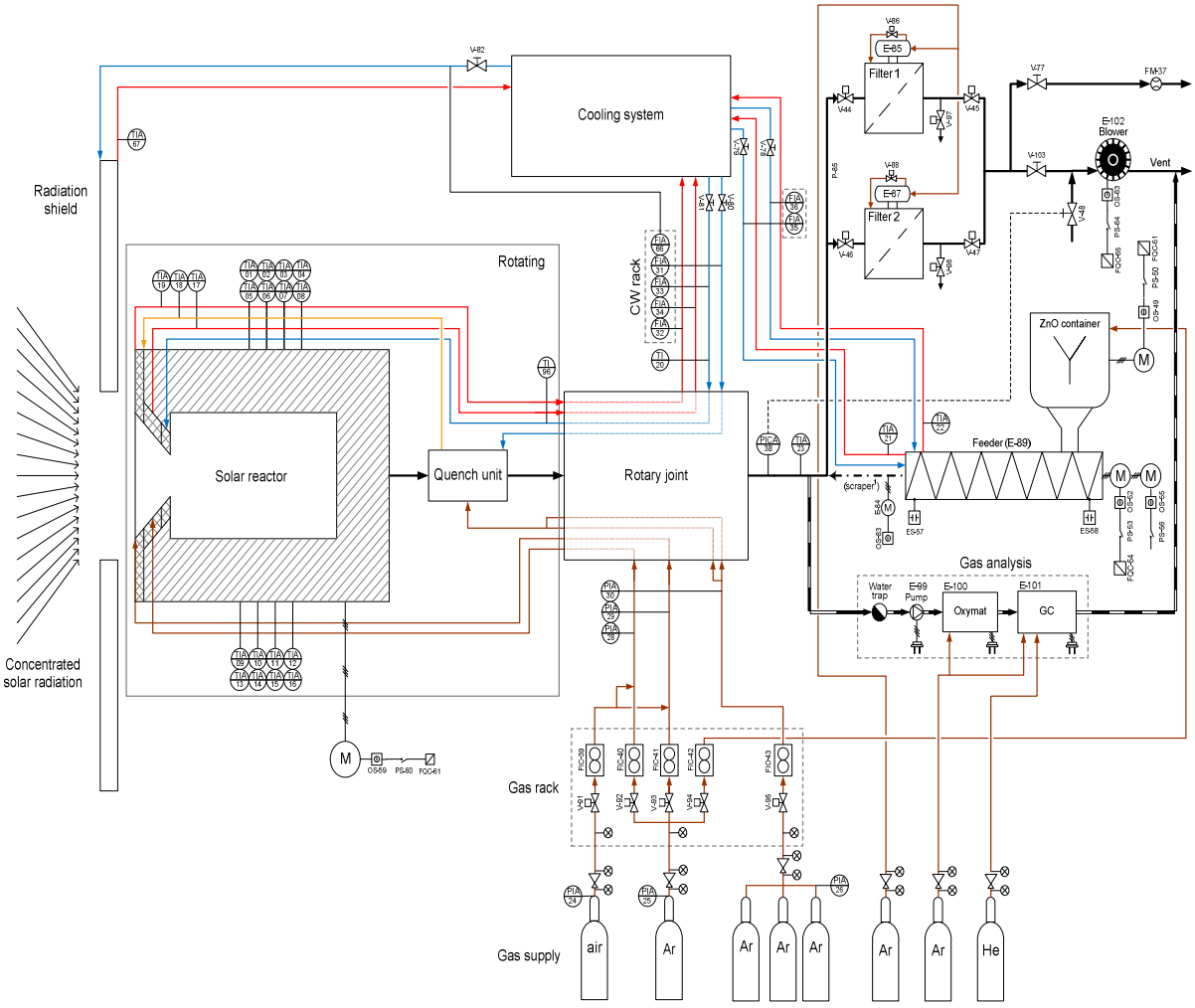

Fig. 4. Piping and instrumentation diagram of the solar pilot plant including radiation shield, solar reactor, quench unit, rotary joint, ZnO dynamic feeder, filter system, pressure control, gas supply and storage, gas analysis, cooling water supply, water and gas piping, and location of temperature and pressure indication.

Gas supply (Ar, synthetic air) to the rotary reactor comprises the window and quench flows being fed through the rotary joint. A further gas stream is used to purge the ZnO container and the screw feeder. Gas flows are set using electronic mass flow controllers (Bronkhorst AG) mounted on the gas rack. Gas bottles and frames are stored outside the solar tower and connected to fixed gas supply lines.

For the product gas analysis, a small gas flow (1.3 l_N/min) is extracted downstream the quench unit through a gas filter (HEPA, pore size 1.2 μm) into a gas chromatograph (Varian CP4900) to determine the exhaust gas composition. Gases including N_2, O_2, H_2, CO, CO_2, and CH_4 may be detected every two minutes approximately.

The filtering system (Hablützel AG, pore size 3 μm) separates solid particles from the exhaust gas, which ideally only contains Ar, low O_2 concentrations, and Zn particles. Switching between two filters using control valves (Valpes) allows collecting particles during the heat-up and cool-down phases separately from those produced at the desired operating temperature. The pressure inside the reactor is kept at 10 mbar (gauge) using a side channel blower (DutchAir) that is installed downstream the filter system. A slanted seat valve (Schubert&Salzer control systems) placed between the filter system and the side channel blower regulates the pressure by opening and closing towards the ambient and subsequently increasing or decreasing the gas flow from the reactor.

Temperatures, pressure, inert gas and cooling water flows are acquired throughout the experimental run. Temperatures are measured with B-type (layer L2, Fig. 2b) and K-type thermocouples (layers L3 and L4, Fig. 2b) placed inside the solar reactor. Gas and cooling water temperatures are observed with Pt-100 temperature sensors.

2.3. Experimental setup

The reactor and all sub-components, apart from the filters and the gas analysis equipment, are installed on a mobile aluminum modular profile system (Bosch Rexroth AG), as shown in Fig. 3. The Bosch profile is mounted on a movable carriage system (2.8 m x 3.2 m) to allow manageable and flexible transport from the ground floor to the solar tower focal point as well as to facilitate on-site maintenance tasks. For the preparation of an experiment, the Bosch profile is retracted to make possible the access to the reactor cavity and ease mounting the window and the reactor front shield. Prior to starting an experimental run, the carriage is being moved forward until the reactor aperture intercepts the focal plane. Cooling water supply to all cooled parts is enabled, while the protective Ar flows through the radial and tangential nozzles are both set to 15 l_N/min.

2.4. Experimental procedure

For a typical experimental run, six center heliostats out of 63 in total (each with a mirror area of 45 m^2) are set into track mode. Subsequently, the shutter doors are opened in small steps to allow steady heat-up and to alleviate thermal stress on the cavity lining. To further increase the radiative power delivered to the solar reactor, more heliostats are set into tracking position (up to 25 heliostats in total, depending on the goal of the experimental run). Once the reference temperature T1 (see Fig. 2b) approaches 1773 K, the filters are swapped and the Ar flow to the quench system is set to 1500 l_N/min. At 1873 K, the feeding routine is started to line the bottom wall of the cavity with a batch of ZnO particles. The reactor is kept at or slightly above this temperature (T1, Fig. 5a) while dissociating ZnO as long as the weather conditions are suitable, Fig.5c.

During the cooling down of the reactor cavity, both Ar flow rates at the window are initially maintained at 15 l_N/min and then reduced to 10 l_N/min as soon as T1 drops below 1273 K. The gas flow is kept running overnight to prevent re-oxidation of the produced Zn(s), and the cooling water is kept flowing to protect the window and quench unit from over-heating.

4. Experimental results

The solar pilot plant was assembled and mounted on the mobile carriage within less than one week. Installation on the experimental platform in the solar tower and commissioning of the complete plant

required another ten days. Functionality tests of all system components included cooling water, gas supply and off-gas piping, electrical and electronic connections, process control and data acquisition systems.

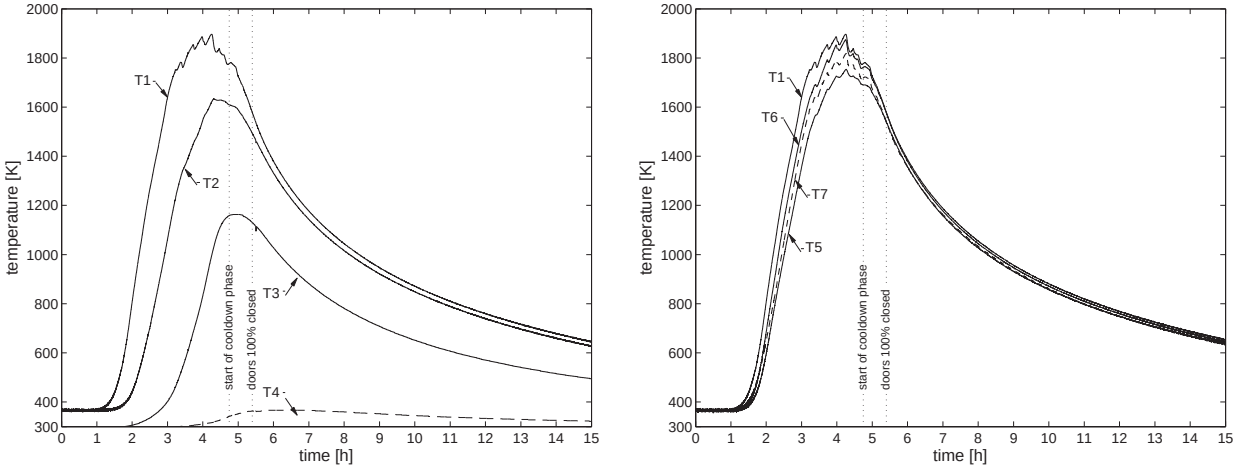

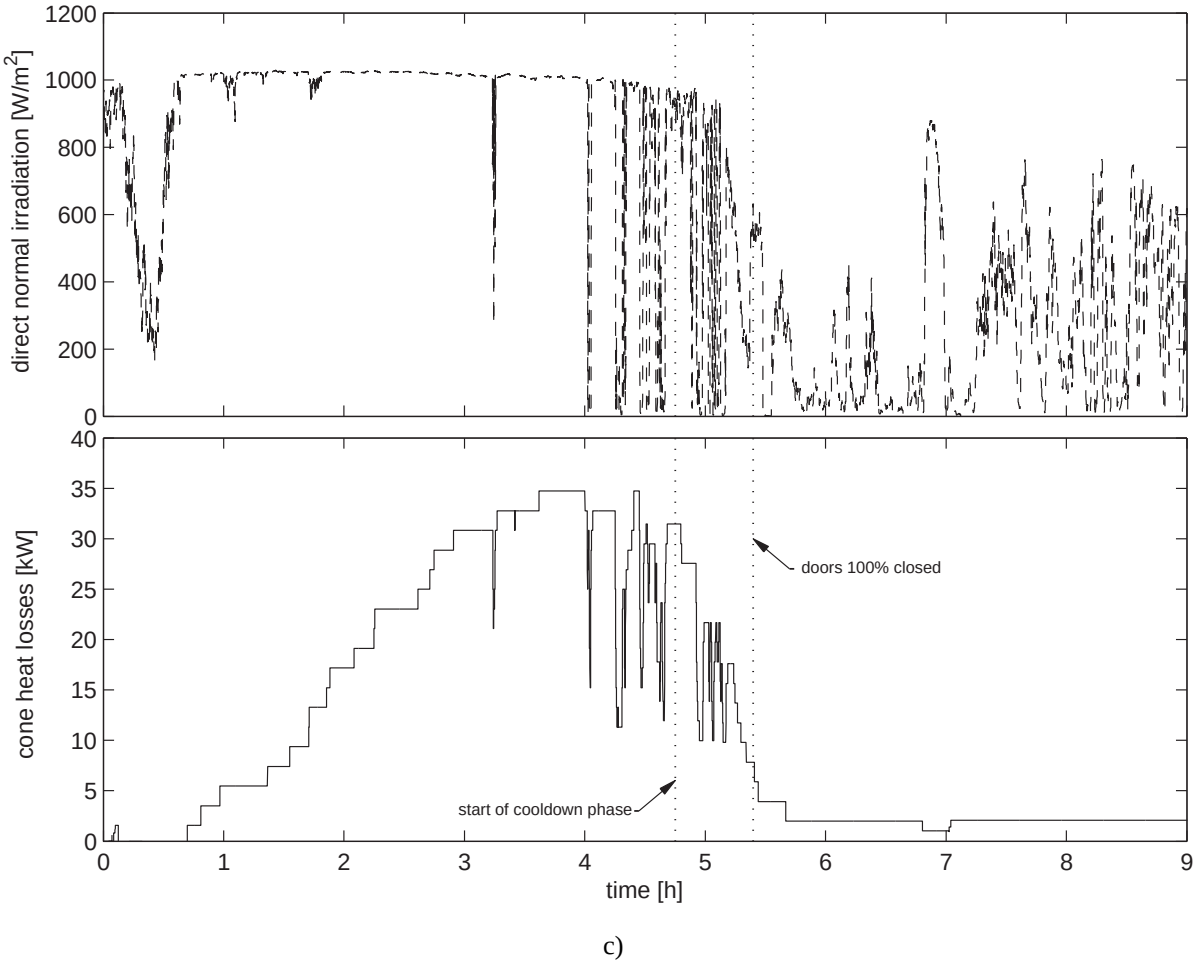

Fig. 5. a) Temperature devolution vs. experimental time for thermocouples at position T1, T2, T3 and T4; b) Temperature devolution vs. experimental time for thermocouples at position T1, T5, T6 and T7; c) Direct normal irradiation (DNI, real-time data provided by PROMES-CNRS) and heat loss at the front cone calculated from the temperature difference of the cooling water flow vs. the experimental time.

Solar experimentation in the MWSF started with slow heating up of the reactor cavity to remove the remnant moisture inside the insulation, which stemmed from the manufacturing process. For that purpose, the window was removed and the feeder was retracted to facilitate the water vapor exiting the reactor. Drying the cavity, however, led to shrinking of the insulation layers and to the formation of gaps between the outer ceramic layer (L4, see Fig. 2b) and the reactor shell. Subsequently, the rotational movement of the reactor imposed mechanical stress on the cavity lining and resulted in alumina tiles being detached. Although the damaged cavity was repaired quickly by gluing the tiles onto the insulation, further runs were performed without rotating the reactor.

Eleven solar experimental runs with more than 60 hours of on-sun testing were performed in the MWSF. Among them were eight heat-up experiments to cure the refractory materials by evaporating residual water within the insulation and removing organic binding compounds. The duration of these experiments was between three and seven hours, and the maximum temperatures reached between 803 K and 1796 K (T1, measured behind the alumina tiles). The last three experimental runs were conducted with the window attached to the reactor front and with the goal to dissociate ZnO and produce solar Zn. The duration of each of these experiments was between five and six hours, and the maximum operational temperature (T1) was between 1873 K and 1903 K. Due to intermittent solar radiation caused by cloud coverage of the sky, most of the experiments were disturbed or had to be stopped untimely.

Figure 5 depicts preliminary results from a typical solar experiment for ZnO dissociation. The temperature devolution with time is shown in Fig. 5a across the cavity insulation for T1 (behind the alumina tiles), T2, T3, and T4 (inside the reactor shell), and in Fig. 5b along the cylindrical cavity lining for T5 (front), T1 (center), T6 (back), and T7 (rear wall). The location of the thermocouples is indicated in Fig. 2b. The highest heating rate reached at T1 was 84.5 K/min. The unsteady behavior close to the maximum temperature (between 4 and 5 hours) is due to clouds, which influenced the direct normal irradiation (DNI, see Fig. 5c) and, thus, the power input to the reactor. The highest cooling rate reached was 5.4 K/min after the power input was completely removed (heliostats on stand-by and doors fully closed). Neither the maximum heating rate nor the maximum cooling rate introduced unmanageable temperature tensions for the ceramic insulation and the alumina tiles contained within the reactor shell.

Figure 5c depicts the heat loss at the front cone calculated from the temperature difference of the cooling water flow vs. the experimental time. Up to 35 kW have to be cooled away at the front cone alone, when the highest power input is reached (doors fully open, 25 heliostats in track mode). At steady state, the heat loss almost instantaneously followed the DNI, which was characterized by intermittent solar radiation due to clouds that eventually impeded continuation of the experiment shortly after starting the ZnO dissociation.

After cooling down the reactor, 42.7 g of solid products consisting of Zn and ZnO was found and recovered from the filter that was used during quenching. The analysis of the recovered powder using the HCl method – i.e., dissolving metallic Zn in dilute hydrochloric acid (HCl) to form zinc chloride ($ZnCl_2$) and H_2 in an exothermic reaction – showed a Zn yield of 45.9 %.

5. Conclusion and outlook

A 100 kW pilot plant for the solar thermal dissociation of ZnO was designed and fabricated at PSI. A first experimental campaign of six weeks was scheduled and conducted in June/July 2011 at the MWSF in Odeillo. More than 60 hours of on-sun testing in the MWSF were recorded, each experiment lasting between three and seven hours. All systems of the solar pilot plant have been tested and qualified. Valuable operational experience with a 100 kW pilot plant was gathered and will help to further improve the current design for the second experimental campaign planned for 2012. It aims at optimizing the reactor performance by implementing a modified quench unit and by operating the reactor at higher temperatures using improved high-temperature wall materials. The goal will be to reach a Zn yield exceeding 50 % and a solar-to-chemical energy conversion efficiency approaching 10 %. The results from this research will extent the ability to store solar energy as a fuel – such as Zn, H_2, or syngas – in a manner that increases the chances of having a sustainable solution to the current world problem of being dependent on a limited supply of fossil fuels.

Acknowledgements

This investigation was financially supported by the Swiss Federal Office of Energy (SFOE). The experimental campaign at the MWSF in Odeillo was partly funded by the European Project SFERA (Solar Facilities for the European Research Area), providing user access through grant agreement No. 228296. The authors are grateful to Y. Baeuerle, A. Frei, D. Meyer, P. Schaller, and D. Wuillemin from the STL-PSI team for technical support, and to E. Guillot, J.-L. Sans, and N. Boullet from PROMES-CNRS for preparing and operating the MWSF.

References

[1] A. Steinfeld and A. Meier, (2004). Solar Fuels and Materials. In: Encyclopedia of Energy, C. Cleveland Ed., Elsevier, Vol. 5, pp. 623-637.

[2] A. Steinfeld, Int. J. Hydrogen Energy, 27 (2002) 611-619.

[3] A. Steinfeld and A. Weimer, Opt. Express, 18 (2010) A100-A111.

[4] W.C. Chueh, C. Falter, M. Abbott, D. Scipio, P. Furler, S.M. Haile and A. Steinfeld, Science, 330 (2010) 1797-1801.

[5] P.G. Loutzenhiser, A. Meier and A. Steinfeld, Materials, 3 (2010) 4922-4938. *doi:10.3390/ma3114922*

[6] D. Gstoehl, A. Brambilla, L.O. Schunk and A. Steinfeld, Journal of Materials Science, 43 (2008) 4729-4736.

[7] L.O. Schunk, W. Lipinski and A. Steinfeld, Chemical Engineering Journal, 150 (2009) 502-508.

[8] F. Trombe and A. Le Phat Vinh, Solar Energy, 15 (1973) 57-61.

[9] R. Müller, P. Haeberling and R. Palumbo, Solar Energy, 80 (2006) 500-511.

[10] R. Müller, W. Lipinski and A. Steinfeld, Applied Thermal Engineering, 28 (2008) 524-531.

[11] L.O. Schunk, P. Haeberling, S. Wepf, D. Wuillemin, A. Meier and A. Steinfeld, J. Solar Energy Eng., 130 (2008) 021009.

[12] M.A. Clevinger, K.M. Hill and C.L. Cedeno (1995) Phase Equilibria Diagrams: Phase Diagrams for Ceramists: 1995 Cumulative Indexes: Volumes 1-11, Annuals ’91-’93, High Tc Monograph, The American Ceramic Society, Westerville, OH.